# Mott Quantum Critical Points at Finite Doping

Maria Chatzieleftheriou,[1] Alexander Kowalski,[2] Maja Berović,[3] Adriano Amaricci,[4] Massimo Capone,[3,4] Lorenzo De Leo,[1] Giorgio Sangiovanni,[2] and Luca de' Medici[1,*]

[1]*Laboratoire de Physique et Etude des Matériaux, UMR8213 CNRS/ESPCI/UPMC, 75005 Paris, France*
[2]*Institut für Theoretische Physik und Astrophysik and Würzburg-Dresden Cluster of Excellence ct.qmat, Universität Würzburg, 97074 Würzburg, Germany*
[3]*International School for Advanced Studies (SISSA), Via Bonomea 265, I-34136 Trieste, Italy*
[4]*CNR-IOM DEMOCRITOS, Istituto Officina dei Materiali, Consiglio Nazionale delle Ricerche, Via Bonomea 265, I-34136 Trieste, Italy*

(Received 2 April 2022; accepted 22 December 2022; published 7 February 2023)

We demonstrate that a finite-doping quantum critical point (QCP) naturally descends from the existence of a first-order Mott transition in the phase diagram of a strongly correlated material. In a prototypical case of a first-order Mott transition the surface associated with the equation of state for the homogeneous system is "folded" so that in a range of parameters stable metallic and insulating phases exist and are connected by an unstable metallic branch. Here we show that tuning the chemical potential, the zero-temperature equation of state gradually unfolds. Under general conditions, we find that the Mott transition evolves into a first-order transition between two metals, associated with a phase separation region ending in the finite-doping QCP. This scenario is here demonstrated solving a minimal multiorbital Hubbard model relevant for the iron-based superconductors, but its origin—the splitting of the atomic ground state multiplet by a small energy scale, here Hund's coupling—is much more general. A strong analogy with cuprate superconductors is traced.

DOI: 10.1103/PhysRevLett.130.066401

Mott physics, charge instabilities, and quantum criticality are recurrent leitmotifs in the field of strongly correlated materials [1]. Their connection [2,3] was explored early on theoretically for the cuprate superconductors [4–7]. These are indeed doped Mott insulators and host both a "strange," possibly quantum critical metal, and incommensurate charge-density wave phases [8,9]. Moreover charge instabilities occur in a variety of other correlated systems like, e.g., titanates [10] and transition-metal dichalcogenides [11]. However despite the great interest in this topic a clear physical picture of the conditions leading to phase separation and quantum criticality in doped Mott insulators is still missing.

In this work we broaden the perspective and show that a phase separation zone ending in a QCP is an intrinsic feature connected to the Mott transition. We address this issue within a different framework, namely, a Hund's metal which is realized in a doped multiorbital Hubbard model. We can thus both build on the recent understanding of Hund's metals triggered by iron-based superconductors [12–16] and attack the problem by solving a simplified model using dynamical mean-field theory (DMFT) [17] in a numerically exact way, ruling out any ambiguity connected with the numerical solution. More specifically we use DMFT solved by the numerical renormalization group (NRG) at zero temperature to study a two-orbital Hubbard model with on-site Coulomb repulsion $U$ and Hund's exchange coupling $J$, which favors high-spin states on every atom [16].

Our study of this simple and paradigmatic model shows that the generic first-order character of the transition for $J \neq 0$ [18–20], which implies two stable solutions, can be linked directly to finite-doping instabilities. We argue that these results are general to a wide class of models where another energy scale besides the Hubbard $U$ is present.

The model we analyze is the degenerate two-orbital Hubbard model in the paramagnetic phase. The Hamiltonian reads

$$\hat{H} = \sum_{i \neq j m\sigma} t_{ij} d^{\dagger}_{im\sigma} d_{jm\sigma} + U \sum_{im} \tilde{n}_{im\uparrow} \tilde{n}_{im\downarrow} + (U - 2J) \sum_{im \neq m'} \tilde{n}_{im\uparrow} \tilde{n}_{im'\downarrow} + (U - 3J) \sum_{im < m', \sigma} \tilde{n}_{im\sigma} \tilde{n}_{im'\sigma} \tag{1}$$

where $d^{\dagger}_{im\sigma}$ creates an electron with spin $\sigma$ in orbital $m = 1, 2$ on site $i$ of the lattice, and $\tilde{n}_{im\sigma} = n_{im\sigma} - 1/2$ is a particle-hole symmetric form of the density operators $n_{im\sigma} = d^{\dagger}_{im\sigma} d_{im\sigma}$. We take $J/U = 0.25$. Our analysis depends on the local many-body physics and not on details of the band structure obtained by diagonalizing the one-body part of the Hamiltonian $\hat{H}_0 - \mu \hat{N} = \sum_{km\sigma} (\epsilon_k - \mu) d^{\dagger}_{km\sigma} d_{km\sigma}$, where $\mu$ is the chemical potential

 

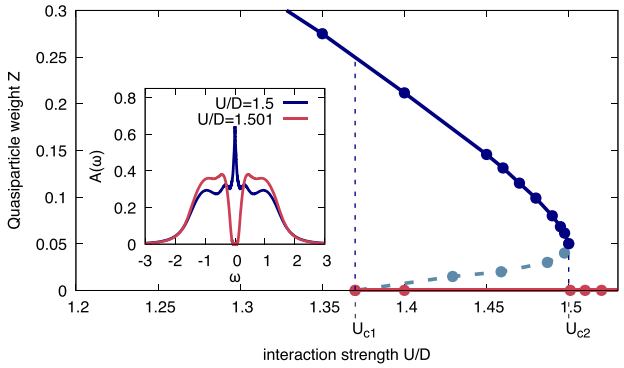


FIG. 1. Multiple solutions close to the Mott transition at $T = 0$: interaction-driven transition. Its first-order character is due to the finite value of Hund's coupling $J$ and is embodied by the sigmoidal shape of the $Z(U)$ curve in the range of interaction strengths $U_{c1} < U < U_{c2}$ where two stable solutions—one metallic at finite $Z$ (blue) and one insulating at $Z = 0$ (red)—coexist, and are connected by a third unstable metallic branch (light blue dashed line). Inset: change of spectral function between the metallic and insulating stable solutions when passing $U_{c2} = 1.5D$.

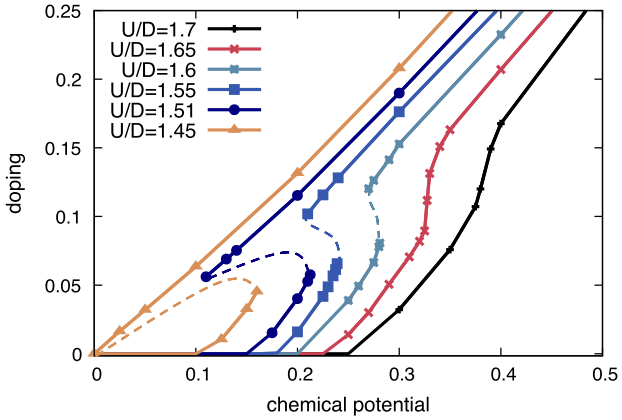


FIG. 2. Multiple solutions close to the Mott transition at $T = 0$: density-driven transition. We plot the density (measured as doping from half-filling) vs chemical potential curves for several values of the interaction strength $U/D$. The Mott insulator is incompressible and is thus indicated by the horizontal plateau at half-filling, while the doped solutions are metallic. The points are calculated within NRG DMFT, the dashed lines sketch the unstable branch connecting the two stable ones, as deduced from calculations within exact-diagonalization(ED)-DMFT (see Supplemental Material [21]). The adiabatic connection of the solutions implies the crossing of the energy between the two stable branches at some $\mu_c(U)$ in the coexistence zone, and thus a discontinuous jump from one to the other (corresponding to a Maxwell construction).

and $\hat{N} = \sum_{im\sigma} n_{im\sigma}$ is the operator counting the total number of particles in the system. Thus we can choose without loss of generality a featureless band structure with semicircular density of states (DOS) $D(\epsilon) = 2\sqrt{1-(\epsilon/D)^2}/(\pi D)$ of half-bandwidth $D$ (corresponding, e.g., to a Bethe lattice with infinite connectivity). With this choice the model is half-filled (i.e., the electron density $n \equiv \sum_{m\sigma}\langle n_{im\sigma}\rangle = 2$) for $\mu = 0$.

We start from the half-filled system. In Fig. 1 we show the zero-temperature quasiparticle weight $Z$, which is a measure of the system's metallicity (see Supplemental Material [21]) and whose vanishing signals the Mott transition. As a function of the interaction strength $U$ the metallic solution does not evolve continuously in the insulating one though, as testified by the sharp change in the spectrum: the gap opens abruptly beyond a threshold value labeled $U_{c2}$, while the central peak—of which $Z$ is the spectral weight—disappears. Importantly, the insulating solution with $Z = 0$ exists not only for all larger values of $U$ but also for a range $U_{c1} < U < U_{c2}$ where the equation of state of the system is then multivalued. The actual transition point $U_c$ is where the energies of the two solutions cross.

A crucial feature is that the two stable solutions are adiabatically connected [18,41,42] through a third, unstable metallic branch joining the stable metallic branch in $U_{c2}$ to the stable insulating branch in $U_{c1}$. This implies that, following by continuity the three solutions, the equation of state is folded into a characteristic sigmoidal shape.

These features have substantial consequences for the doped system, which corresponds to a finite chemical potential $\mu$ (our model being half-filled for $\mu = 0$). The two solutions evolve differently with $\mu$ [3]. Indeed as shown in Fig. 2 they turn into coexisting stable solutions with different densities $n$ for the same value of $\mu$. Yet they retain their adiabatic connection, giving rise to a sigmoidal shape for the $n(\mu)$ curve, which implies the existence of a zone of phase separation. One can overall visualize [Figs. 3(a) and 3(b)] the equation of state as a surface in three dimensions which is folded in a zone of the $U$-$\mu$ plane.

On the other hand, at large doping (large $\mu$) one can expect that all the fingerprints of Mott physics are washed away and a standard metal is recovered. This implies a complete "unfolding" of the equation of state at some $\mu$ after which the system is single valued as a function of thermodynamic parameters (here $U$ and $\mu$). Since the paramagnetic Mott insulator can only be realized at integer filling, a possible outcome is that the threshold $\mu$ corresponds to an infinitesimal doping. Our results show instead a different scenario where the two stable solutions survive at finite doping and they all have metallic character. As a consequence, the equation of states unfolds at a finite doping, leading to a finite-doping quantum critical point.

Calculated $n(\mu)$ curves for several values of $U$ are reported in Fig. 2. For all values $U_{c1} < U < U_{c2}$ (e.g., for $U/D = 1.45$—yellow curve in the figure) the two stable solutions existing at half-filling continue at finite $\mu$: the metallic solution is immediately doped while the insulating solution remains pinned at half-filling for a finite range of the chemical potential (corresponding to the gap of the

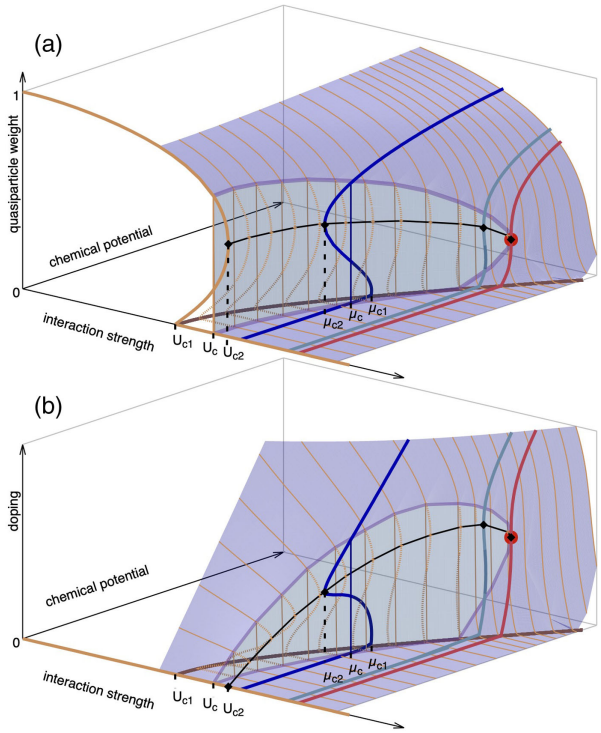


FIG. 3. Folding of the equation of state. (a) Illustration of the dependence of the quasiparticle weight $Z$ as a surface plot, as a function of the position in the $U$-$\mu$ plane. The golden line at $\mu = 0$ corresponds to the interaction-driven Mott transition at half-filling (Fig. 1). (b) Corresponding surface plot of the density (doping from half-filling). Curves are plotted corresponding roughly to those of Fig. 2. The vertical light blue surface corresponds to the Maxwell construction (and physically defines the zone of phase separation) and illustrates the continuity, and common first-order nature, between the interaction-driven Mott transition, the density-driven one in the range near $U_{c1}$ and $U_{c2}$, and the transition between two metals ending in a QCP. This whole scenario is entailed by the folding of the equation of state surface as a multivalued function on the $U$-$\mu$ plane (thin golden lines).

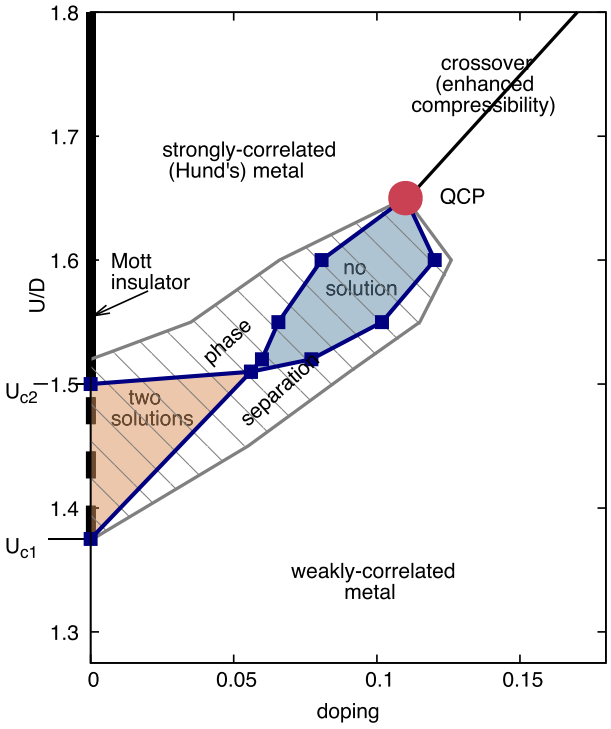


FIG. 4. Zero-temperature phase diagram in the interaction strength-doping plane. The thick black line at half-filling is the Mott insulating phase. The dashed black line signals its coexistence with a metal at half-filling. The density-driven Mott transition is first order for $U_{c1} < U \lesssim U_{c2}$, due to the first-order nature of the interaction-driven Mott transition, and is accompanied by a zone of phase separation (in this zone, for any given value of $U$, the stable phase of the system is a mixture of the two homogeneous phases located at the border of the zone for the same $U$, in proportions needed to obtain the system's doping—its frontier starts at $U_{c1}$ and terminates near, but not exactly at, $U_{c2}$, see Supplemental Material [21]). For larger interaction strengths the first-order transition is realized between two metals, whereas the density-driven Mott transition becomes second order.

Mott insulator) and eventually becomes doped too. However, this doped Mott insulator is a different metal from the continuation of the half-filled metal: both are Fermi liquids (see Supplemental Material [21]) but the former has a much smaller quasiparticle weight, and much lower coherence temperature [43].

As we mentioned above, the two stable branches are connected through an unstable solution which implies that the boundaries of the two branches are two spinodal lines where the electronic compressibility $\kappa = (1/n^2)(dn/d\mu)$ diverges. This also implies the crossing of the free energies of the two stable solutions at some value of the chemical potential $\mu_c$ in the coexistence range, which then corresponds to a Maxwell construction [see Figs. 3(a) and 3(b)]. This determines the first-order nature of the density-driven Mott transition in a range of interactions $U_{c1} < U \lesssim U_{c2}$, which follows from the first-order nature of the interaction-driven transition and the continuity of the equation of state. The spinodal lines and the approximate phase separation zone are reported in Fig. 4.

For $U > U_{c2}$ no metallic solution exists at half-filling and the coexistence zone shifts to larger values of $\mu$, and is seen to shrink (blue curves in Fig. 2). The Maxwell construction jump will then eventually happen at a $\mu_c$ where both branches are metallic. Therefore the discontinuous Mott transition evolves in a discontinuous transition between two differently doped metals. In contrast, for these (and all larger) values of $U$, the actual doping-driven Mott metal-insulator transition becomes second order.

Finally, we find that when $U$ grows beyond a critical value $U_{\mathrm{QCP}}$ the sigmoid straightens (red curve in Fig. 2), the unstable solution disappears and two stable branches merge into one continuous stable solution. This allows us to establish the existence of a quantum critical point (QCP)

at finite doping, where the two spinodals of the zero-temperature first-order transition merge. There, $dn/d\mu$, thus the electronic compressibility $\kappa$, diverges. For $U > U_{\mathrm{QCP}}$ we are left with a smooth crossover. However, the $\mu$ vs $n$ curve retains an inflection point (black curve in Fig. 2), hence a maximum of the compressibility which culminates in the divergence at the QCP.

This confirms and substantiates the scenario of Refs. [44] and [45], where in general a "moustache"-shaped zone of phase separation, delimited by a diverging compressibility and departing from the Mott transition point, crosses the $U$-doping phase diagram of the Hund's metals.

It was also shown earlier in Ref. [3] that the incompressible insulating solution emerging from a first-order Mott transition generally crosses its energy again with the coexisting metallic solution at some finite $\mu$, implying a first-order density-driven Mott transition and phase separation. We crucially modify and extend this picture here with the continuity between the two solutions, which implies the existence of spinodals limiting the coexistence zone and the phase separation to a small range of $U$, and with the unfolding of the continuous solution leading to a QCP.

As a matter of fact, the model we solved realizes a zero-temperature analog of the liquid-gas transition, the role of temperature and pressure being played here by the chemical potential and the interaction strength.

However, this scenario holds only at finite Hund's coupling. At $J = 0$ the transition becomes second order at zero temperature everywhere, and no QCP is realized at finite doping, similarly to the single-band case [46–50]. The key point allowing for the present scenario of phase separation culminating in a QCP is thus the sigmoidal form of the doping-vs-$\mu$ curve at $T = 0$, which is ultimately caused by the first-order character of the interaction-driven Mott transition at half-filling. A natural question thus is, Why does the onset of Hund's coupling cause this transition to become first order? How general is the mechanism?

We can get this insight through the analysis of the present model in the slave-spin mean-field approximation (SSMF—see Supplemental Material [21]) [51], which is similar to DMFT, but yields simplified yet reliable physics, and here is analytically tractable. This method describes the system as a Fermi liquid with quasiparticle weight $Z$ computed from an auxiliary system of quantum spins on a lattice, where it is proportional to the square of the $x$ component of their total on-site magnetization, $m_x$. The Mott transition maps then onto a ferromagnetic-to-paramagnetic transition of the auxiliary system where $\sqrt{Z} \propto m_x$ plays the role of the order parameter.

The structure of the competing solutions can be analyzed within a Landau theory, by coupling a fictitious external magnetic field $h_{\mathrm{ext}}$ conjugated to $m_x$. The behavior of the numerically calculated Landau energy function (see Supplementary Material [21]) $\Gamma(m_x)$ (Fig. 5) clearly illustrates the first order nature of the transition.

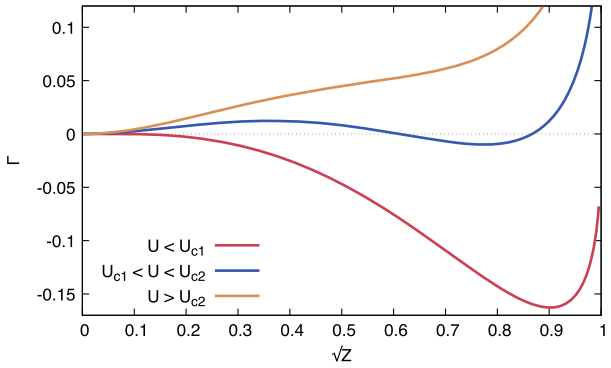


FIG. 5. Landau theory of the first-order Mott transition. Landau energy function calculated within the slave-spin mean field (SSMF), where the extrema indicate the stable (minima) and unstable (maxima) equilibrium solutions for the order parameter $m_x/M = \sqrt{Z}$ (where $M$ is the number of orbitals, here $M = 2$, and $Z$ is the quasiparticle weight) for various values of $U$ at half-filling (see Fig. 1): below $U_{c1}$ (one minimum at large $Z$, corresponding to a metal), in the coexistence zone $U_{c1} < U < U_{c2}$ (two minima—one of which at $Z = 0$, corresponding to the Mott insulator—and one maximum in between), and above $U_{c2}$ (one minimum in $Z = 0$).

We can calculate $\Gamma(m_x)$ analytically in the vicinity of a Mott insulator, that is around $m_x = 0$, where $\Gamma(m_x) = \gamma_2 m_x^2 + \gamma_4 m_x^4 + O(m_x^6)$. In order to have the double-minimum structure needed for a first-order transition $\gamma_4$ has to be negative when $\gamma_2$ goes from negative to positive for increasing $U$ (which then marks $U_{c1}$ in our case). We do find that $\gamma_4 < 0$ for every $J < U$ in this model, and we can attach a physical meaning to this result.

Indeed it can be easily shown (see Supplemental Material [21]) that $\gamma_4$ has the same sign of the coefficient $e_4$ in the perturbative expansion of the slave-spin ground state energy $E = e_2\tilde{h}^2 + e_4\tilde{h}^4 + O(\tilde{h}^6)$, in terms of the field (self-consistent + external) $\tilde{h}$ acting on each spin. In absence of the perturbation ($\tilde{h} = 0$), the slave-spin Hamiltonian reproduces the local atomic spectrum (Fig. 6). In the half-filled sector (in which the electrons are $N = M = 2$, M being the number of orbitals) the states are split by the Hund's coupling $J$, while their distance with the sectors with $N = 3$ and $N = 1$ is $(U + J)/2$. The perturbation changes the occupation, so $e_4$ is due to all the processes involving four hops between neighboring sectors. These processes can be connected (four consecutive jumps starting from and ending in the ground state, but not going through it otherwise—in Fig. 6 these are indicated by the arrows in the order "$a$-$b$-$b$-$a$"), or disconnected (products of lower-order processes—a round–trip on the "$a$" arrows), weighted at the denominator by the energy distance of each intermediate state from the ground state. The connected contributions are always negative while the others are positive at the fourth order. Now, in the present case only the connected contributions can visit the excited

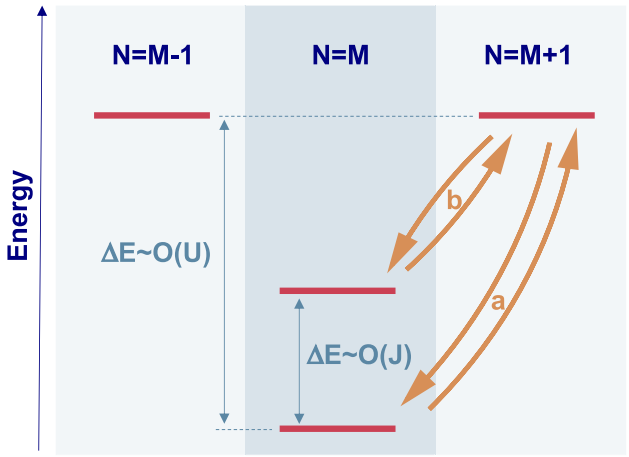


FIG. 6. Landau theory of the first-order Mott transition. Sketch of the main features of the atomic spectrum (see Fig. S9 in the Supplemental Material [21] for the complete spectrum) and hopping processes involved in the strong-coupling perturbation theory giving the fourth-order correction to the ground-state energy $e_4$, which determines the order of the interaction-driven Mott transition. In our model at half-filling the spectrum is symmetric with respect to the half-filled sector (number of electrons $N = M$). The connected process "$a$-$b$-$b$-$a$" is negative in sign and its denominator involves a small energy difference $\sim O(J)$ due to the visiting of an excited state in the $N = M$ sector, and thus dominates over the positive lower-order processes (back and forth on the "$a$" arrows) whose denominators are $\sim O(U)$. This entails a negative $e_4$ and in turn a negative fourth order coefficient $\gamma_4$ in the Landau energy (see text), thus a first-order Mott transition.

states in the $N = 2$ sector, at distance $J$ in energy from the ground state, thus involving a small denominator. Taking into account all the possible processes they turn out to dominate on the disconnected contributions that involve only the larger energy difference $\sim O(U)$. This causes $e_4$ and thus $\gamma_4$ to be negative.

Hence the ultimate cause of a first-order Mott transition is a splitting of the atomic ground-state multiplet much smaller than the energy cost of charge excitations [52]. We can also argue that essentially any term breaking the SU (2M) symmetry leads to the same picture, including, e.g., a Jahn-Teller distortion [53] or a crystal field splitting.

The scenario linking a first-order Mott transition with phase separation and quantum criticality naturally calls for a connection with models for the cuprates [15,54]. In that context, phase separation appears ubiquitously in two-dimensional strongly correlated models [4,5,7]. In particular cluster dynamical mean-field theory (CDMFT) studies have shown an enhancement of the compressibility at finite temperature culminating with an instability zone which marks the entrance into the pseudogap phase [55]. This finite-doping instability causes a first-order transition between two metals across a frontier which can be tracked back to the Mott transition at half-filling, in close analogy with the present analysis. We can thus speculate that this zone ends in a QCP at a critical value of the interaction [56] providing us with a straightforward scenario that connects the indubitable Mott physics with the very existence of a QCP.

The authors are grateful to Rok Zitko for insightful exchanges and to Jakob Steinbauer for sharing some of his data. L. d M. thanks J. Lorenzana and M. Schirò for useful discussions. M. Ch., and L. d. M. are supported by the European Commission through the ERC-CoG2016, StrongCoPhy4Energy, GA No. 724177. A. K. and G. S. were supported by the Deutsche Forschungsgemeinschaft (DFG, German Research Foundation) through Project-ID 258499086—SFB 1170 and through the Würzburg-Dresden Cluster of Excellence on Complexity and Topology in Quantum Matter ct.qmat (Project-ID 390858490, EXC 2147) and gratefully acknowledge the Gauss Centre for Supercomputing e. V. [57] for funding this project by providing computing time at the Leibniz Supercomputing Centre [58]. M. B. and M. C. acknowledge support of the Italian MIUR through PRIN 2015 (Prot. 2015C5SEJJ001) and PRIN 2017 CenTral.

*Corresponding author.
luca.demedici@espci.fr

[1] M. Imada, A. Fujimori, and Y. Tokura, Metal-insulator transitions, Rev. Mod. Phys. **70**, 1039 (1998).
[2] C. Castellani, C. Di Castro, D. Feinberg, and J. Ranninger, New Model Hamiltonian for the Metal-Insulator Transition, Phys. Rev. Lett. **43**, 1957 (1979).
[3] C.-H. Yee and L. Balents, Phase Separation in Doped Mott Insulators, Phys. Rev. X **5**, 021007 (2015).
[4] V. J. Emery, S. A. Kivelson, and H. Q. Lin, Phase Separation in the t-j Model, Phys. Rev. Lett. **64**, 475 (1990).
[5] M. Grilli, R. Raimondi, C. Castellani, C. Di Castro, and G. Kotliar, Superconductivity, Phase Separation, and Charge-Transfer Instability in the u = ∞ Limit of the Three-Band Model of the cuo$_2$ Planes, Phys. Rev. Lett. **67**, 259 (1991).
[6] C. Castellani, C. Di Castro, and M. Grilli, Singular Quasiparticle Scattering in the Proximity of Charge Instabilities, Phys. Rev. Lett. **75**, 4650 (1995).
[7] N. Furukawa and M. Imada, Two-dimensional Hubbard model—metal insulator transition studied by monte carlo calculation, J. Phys. Soc. Jpn. **61**, 3331 (1992).
[8] R. Arpaia and G. Ghiringhelli, Charge order at high temperature in cuprate superconductors, J. Phys. Soc. Jpn. **90**, 111005 (2021).
[9] M. Imada, Charge order and superconductivity as competing brothers in cuprate high-tc superconductors, J. Phys. Soc. Jpn. **90**, 111009 (2021).
[10] H. D. Zhou and J. B. Goodenough, Coexistence of two electronic phases in latio$_{3+\delta}$($0.01 \leq \delta \leq 0.12$) and their evolution with $\delta$, Phys. Rev. B **71**, 165119 (2005).
[11] B. Sipos, A. F. Kusmartseva, A. Akrap, H. Berger, L. Forró, and E. Tutiš, From Mott state to superconductivity in 1t-tas2, Nat. Mater. **7**, 960 (2008).

[12] Z. P. Yin, K. Haule, and G. Kotliar, Kinetic frustration and the nature of the magnetic and paramagnetic states in iron pnictides and iron chalcogenides, Nat. Mater. **10**, 932 (2011).
[13] P. Werner, E. Gull, M. Troyer, and A. J. Millis, Spin Freezing Transition and Non-Fermi-Liquid Self-Energy in a Three-Orbital Model, Phys. Rev. Lett. **101**, 166405 (2008).
[14] H. Ishida and A. Liebsch, Fermi-liquid, non-fermi-liquid, and Mott phases in iron pnictides and cuprates, Phys. Rev. B **81**, 054513 (2010).
[15] L. de' Medici, G. Giovannetti, and M. Capone, Selective Mott Physics as a Key to Iron Superconductors, Phys. Rev. Lett. **112**, 177001 (2014).
[16] A. Georges, L. de' Medici, and J. Mravlje, Strong correlations from hund's coupling, Annu. Rev. Condens. Matter Phys. **4**, 137 (2013).
[17] A. Georges, G. Kotliar, W. Krauth, and M. J. Rozenberg, Dynamical mean-field theory of strongly correlated fermion systems and the limit of infinite dimensions, Rev. Mod. Phys. **68**, 13 (1996).
[18] Y. Ono, M. Potthoff, and R. Bulla, Mott transitions in correlated electron systems with orbital degrees of freedom, Phys. Rev. B **67**, 035119 (2003).
[19] T. Pruschke and R. Bulla, Hund's coupling and the metal-insulator transition in the two-band Hubbard model, Eur. Phys. J. B **44**, 217 (2005).
[20] K. Hallberg, D. J. García, P. S. Cornaglia, J. I. Facio, and Y. Núñez-Fernández, State-of-the-art techniques for calculating spectral functions in models for correlated materials, Europhys. Lett. **112**, 17001 (2015).
[21] See Supplemental Material at http://link.aps.org/supplemental/10.1103/PhysRevLett.130.066401 for technical details on the methods and comparison between the impurity solvers, discussion on the Fermi-liquid nature of the metallic phases, discussion of the rotationally invariant case, details on the Maxwell construction, detailed treatment of the perturbative expansion of the slave-spin equations, results for a five-orbital model, which includes Refs. [22–40].
[22] R. Bulla, T. A. Costi, and T. Pruschke, Numerical renormalization group method for quantum impurity systems, Rev. Mod. Phys. **80**, 395 (2008).
[23] M. Caffarel and W. Krauth, Exact Diagonalization Approach to Correlated Fermions in Infinite Dimensions: Mott Transition and Superconductivity, Phys. Rev. Lett. **72**, 1545 (1994).
[24] E. Gull, A. J. Millis, A. I. Lichtenstein, A. N. Rubtsov, M. Troyer, and P. Werner, Continuous-time monte carlo methods for quantum impurity models, Rev. Mod. Phys. **83**, 349 (2011).
[25] M. Wallerberger, A. Hausoel, P. Gunacker, A. Kowalski, N. Parragh, F. Goth, K. Held, and G. Sangiovanni, w2dynamics: Local one- and two-particle quantities from dynamical mean field theory, Comput. Phys. Commun. **235**, 388 (2019).
[26] R. Žitko and T. Pruschke, Energy resolution and discretization artifacts in the numerical renormalization group, Phys. Rev. B **79**, 085106 (2009).
[27] A. Weichselbaum and J. von Delft, Sum-Rule Conserving Spectral Functions from the Numerical Renormalization Group, Phys. Rev. Lett. **99**, 076402 (2007).
[28] R. Bulla, A. C. Hewson, and T. Pruschke, Numerical renormalization group calculations for the self-energy of the impurity anderson model, J. Phys. Condens. Matter **10**, 8365 (1998).
[29] A. Amaricci, L. Crippa, A. Scazzola, F. Petocchi, G. Mazza, L. de Medici, and M. Capone, Edipack: A parallel exact diagonalization package for quantum impurity problems, Comput. Phys. Commun. **273**, 108261 (2022).
[30] M. Chatzieleftheriou, Charge instabilities, Mott transition and transport in Hund metals, Ph.D. thesis, PSL University, Paris, 2021.
[31] P. Nozières, A "fermi-liquid" description of the kondo problem at low temperatures, J. Low Temp. Phys. **17**, 31 (1974).
[32] L. de Leo, Non-Fermi liquid behavior in multi-orbital Anderson impurity models and possible relevance for strongly correlated lattice models, Ph.D. thesis, SISSA, 2004.
[33] K. M. Stadler, A model study of strong correlations in hund metals, PhD Thesis, Ludwig-Maximilians-Universität München (2019).
[34] G. Moeller, V. Dobrosavljević, and A. E. Ruckenstein, Rkky interactions and the Mott transition, Phys. Rev. B **59**, 6846 (1999).
[35] H. B. Callen, *Thermodynamics and an Introduction to Thermostatistics*, 2nd ed. (Wiley, New York, NY, 1985).
[36] L. de'Medici, A. Georges, and S. Biermann, Orbital-selective Mott transition in multiband systems: Slave-spin representation and dynamical mean-field theory, Phys. Rev. B **72**, 205124 (2005).
[37] G. Kotliar and A. E. Ruckenstein, New Functional Integral Approach to Strongly Correlated Fermi Systems: The Gutzwiller Approximation as a Saddle Point, Phys. Rev. Lett. **57**, 1362 (1986).
[38] J. W. Negele and H. Orland, *Quantum many-particle systems* (Addison-Wesley, Reading, MA, 1988).
[39] A. Klejnberg and J. Spalek, Simple treatment of the metal-insulator transition: Effects of degeneracy, temperature, and applied magnetic field, Phys. Rev. B **57**, 12041 (1998).
[40] F. Lechermann, A. Georges, G. Kotliar, and O. Parcollet, Rotationally invariant slave-boson formalism and momentum dependence of the quasiparticle weight, Phys. Rev. B **76**, 155102 (2007).
[41] H. U. R. Strand, A. Sabashvili, M. Granath, B. Hellsing, and S. Östlund, Dynamical mean field theory phase-space extension and critical properties of the finite temperature Mott transition, Phys. Rev. B **83**, 205136 (2011).
[42] N.-H. Tong, S.-Q. Shen, and F.-C. Pu, Mott-Hubbard transition in infinite dimensions, Phys. Rev. B **64**, 235109 (2001).
[43] J. Steinbauer, L. de' Medici, and S. Biermann, Doping-driven metal-insulator transition in correlated electron systems with strong hund's exchange coupling, Phys. Rev. B **100**, 085104 (2019).
[44] L. de' Medici, Hund's Induced Fermi-Liquid Instabilities and Enhanced Quasiparticle Interactions, Phys. Rev. Lett. **118**, 167003 (2017).
[45] M. Chatzieleftheriou, M. Berović, P. Villar Arribi, M. Capone, and L. de' Medici, Enhancement of charge instabilities in hund's metals by breaking of rotational symmetry, Phys. Rev. B **102**, 205127 (2020).

[46] G. Kotliar, S. Murthy, and M. J. Rozenberg, Compressibility Divergence and the Finite Temperature Mott Transition, Phys. Rev. Lett. **89**, 046401 (2002).
[47] M. Eckstein, M. Kollar, M. Potthoff, and D. Vollhardt, Phase separation in the particle-hole asymmetric Hubbard model, Phys. Rev. B **75**, 125103 (2007).
[48] J. Vučičević, H. Terletska, D. Tanasković, and V. Dobrosavljević, Finite-temperature crossover and the quantum Widom line near the Mott transition, Phys. Rev. B **88**, 075143 (2013).
[49] H. Eisenlohr, S.-S. B. Lee, and M. Vojta, Mott quantum criticality in the one-band Hubbard model: Dynamical mean-field theory, power-law spectra, and scaling, Phys. Rev. B **100**, 155152 (2019).
[50] M. Reitner, P. Chalupa, L. Del Re, D. Springer, S. Ciuchi, G. Sangiovanni, and A. Toschi, Attractive Effect of a Strong Electronic Repulsion: The Physics of Vertex Divergences, Phys. Rev. Lett. **125**, 196403 (2020).
[51] L. de' Medici and M. Capone, Modeling many-body physics with Slave-Spin Mean-Field: Mott and Hund's physics in fe-superconductors, in *The Iron Pnictide Superconductors: An Introduction and Overview*, edited by F. Mancini and R. Citro (Springer International Publishing, Cham, 2017), pp. 115–185, 10.1007/978-3-319-56117-2_4.
[52] J. I. Facio, V. Vildosola, D. J. García, and P. S. Cornaglia, On the nature of the Mott transition in multiorbital systems, Phys. Rev. B **95**, 085119 (2017).
[53] M. Capone, M. Fabrizio, C. Castellani, and E. Tosatti, Strongly Correlated Superconductivity and Pseudogap Phase Near a Multiband Mott Insulator, Phys. Rev. Lett. **93**, 047001 (2004).
[54] P. Werner, S. Hoshino, and H. Shinaoka, Spin-freezing perspective on cuprates, Phys. Rev. B **94**, 245134 (2016).
[55] G. Sordi, K. Haule, and A. M. S. Tremblay, Finite Doping Signatures of the Mott Transition in the Two-Dimensional Hubbard Model, Phys. Rev. Lett. **104**, 226402 (2010).
[56] D. Galanakis, E. Khatami, K. Mikelsons, A. Macridin, J. Moreno, D. A. Browne, and M. Jarrell, Quantum criticality and incipient phase separation in the thermodynamic properties of the Hubbard model, Phil. Trans. R. Soc. A **369**, 1670 (2011).
[57] www.gauss-centre.eu.
[58] Computing time on the GCS Supercomputer SuperMUC-NG www.lrz.de.